

High-Order Harmonic Generation and Molecular Orbital Tomography: Characteristics of Molecular Recollision Electronic Wave Packets

Y. Chen^{1,2}, Y. Li³, S. Yang³ and J. Liu^{2,4}

1. Graduate School, China Academy of Engineering Physics,
P.O. Box 8009-30, Beijing, 100088, P. R. China

2. Institute of Applied Physics and Computational Mathematics, P.O. Box 100088, Beijing, P. R. China

3. Department of Physics, Hebei Normal University, Shijiazhuang, 050016, P. R. China

4. Center for Applied Physics and Technology, Peking University, 100084, Beijing, P. R. China

(Dated: November 15, 2018)

We investigate the orientation dependence of molecular high-order harmonic generation (HHG) both numerically and analytically. We show that the molecular recollision electronic wave packets (REWPs) in the HHG are closely related to the ionization potential as well as the particular orbital from which it ionized. As a result, the spectral amplitude of the molecular REWP can be significantly different from its reference atom (i.e., with the same ionization potential as the molecule under study) in some energy regions due to the interference between the atomic cores of the molecules. This finding is important for molecular orbital tomography using HHG [Nature **432**, 867(2004)].

PACS numbers: 42.65.Ky, 32.80.Rm

The orientation dependence of molecular high-order harmonic generation (HHG) in strong laser fields constantly attracts attention in both experiment and theory [1, 2, 3, 4, 5, 6, 7, 8]. A new surge was brought on by the recent emergence of its important application in molecular orbital tomography. Itatani *et al* showed that through calibrating the recollision electronic wave packet (REWP) by a reference atom, the orientation dependence can be used to reconstruct the shape of the highest occupied molecular orbital (HOMO) [9]. The molecular orbital tomography is based on the assumptions that, i) a reference atom exists that is mainly characterized by an ionization potential close to that of the molecule and, ii) the spectral amplitude of the REWP for the reference atom is always identical to that of the molecule, independent of the alignment of the molecule [9, 10, 11, 12, 13]. Investigation of the foundations of molecular orbital tomography has led to valuable insights into the mechanism of atomic and molecular HHG. For example, Levesque *et al.* [14] conjectures a universality in the behavior of atomic HHG spectra scaled by the recombination transition atomic dipole moment. This conjecture and many other assumptions connected to the idea of molecular orbital tomography call for a thorough theoretical examination.

In the present paper, we directly examine the second assumption by numerically calculating the spectral amplitudes for 1D and 2D H_2^+ molecular ions with different internuclear distances and laser intensities. Through comparison with reference atoms that share the same ionization potential, we find that the REWP of H_2^+ is strongly dependent on its orientation in certain energy regimes where the interference between the two atomic cores of the molecules dominates [15]. Analytically, we apply the Lewenstein theory to N_2 and CO_2 molecules that have different HOMOs and internuclear distances. Our theoretical calculations validate the assumption for N_2 in the plateau region of the harmonic spectra that

are of most crucial for tomographic reconstruction of the orbital. But, our calculations invalidate the assumption for CO_2 , showing a strong orientation dependence of the spectra in the plateau region due to the interference. This finding suggests that for molecules such as CO_2 , to accurately reconstruct its orbital using the HHG, the interference effects need to be considered.

The Hamiltonian of H_2^+ or hydrogen-like atoms studied here is $H(t) = \mathbf{p}^2/2 + V(\mathbf{r}) - \mathbf{r} \cdot \mathbf{E}(t)$, with soft-Coulomb potential $V(x) = \frac{-Z}{\sqrt{1.44+(x+R/2)^2}} + \frac{-Z}{\sqrt{1.44+(x-R/2)^2}}$ and $V(x, y) = \frac{-Z}{\sqrt{0.5+(x+R/2)^2+y^2}} + \frac{-Z}{\sqrt{0.5+(x-R/2)^2+y^2}}$ for the 1D and 2D case, respectively, where Z is the effective charge, R is the internuclear separation for H_2^+ , and $R = 0$ a.u. corresponds to the hydrogen-like atom, (for $Z = 1$ and $R = 2$ a.u., the ground state energy for H_2^+ reproduced here is $E_0 = 1.11$ a.u. in both cases). $\mathbf{E}(t)$ is the external electric field. Here, we suppose that the molecular axis is coincident with the x-axis and the external field is linearly polarized with an orientation angle of θ to the molecular axis. In the following calculations, the atom units of $\hbar = e = m_e = 1$ are adopted. Our calculation will be performed for 780 nm trapezoidally shaped laser pulses with a total duration of 10 optical cycles and linear ramps of three optical cycles. Numerically, the above Schrödinger equation is solved by the operator-splitting method. The fast Fourier transform (FFT) is employed to transform the wave function between the position representation and the momentum representation. The boundary is set as ± 200 a.u. and the grid number is 4096. The ground state is obtained by propagation in imaginary time. The numerical convergence is checked with using a finer grid. The coherent part of the harmonic spectrum is obtained from the Fourier transformed dipole acceleration expectation value, and only the harmonics polarized parallel to the incoming field are considered [5].

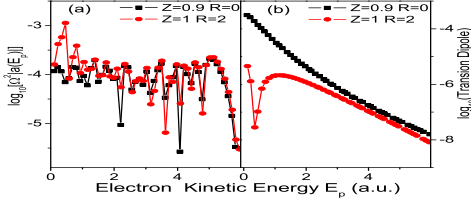


Figure 1: (Color online) The spectral amplitudes $\Omega^2 |a(E_p)| = \sqrt{S(\Omega)}/|\mathbf{d}|$ (a) and transition dipoles $|\langle 0|x|\mathbf{p}\rangle|^2$ (b) of 1D H_2^+ (the red lines) and its reference atom (the black lines) with the continuum $|\mathbf{p}\rangle$ obtained by the numerical method.

According to Ref.[9], the spectral amplitude $a(E_p)$ is

$$|a(E_p)| = \sqrt{S(\Omega)}/2\pi\Omega^2|\mathbf{d}|, \quad (1)$$

where $\mathbf{d}(\mathbf{p}) = \langle \mathbf{p}|\mathbf{r}|0\rangle$ is the transition dipole matrix element of the atom or molecule between the ground state $|0\rangle$ and the continuum state $|\mathbf{p}\rangle$, $S(\Omega)$ is the radiated harmonic signal, Ω is the photon energy, and $E_p = \mathbf{p}^2/2$ is the electronic kinetic energy with $\Omega = E_p + I_p$. I_p is the ionization potential of the atom or molecule.

Fig. 1(a) plots the spectral amplitudes $|a(E_p)|$ of 1D H_2^+ with $Z=1, R=2$ a.u. and its reference atom with $Z=0.9, R=0$ a.u., where $|a(E_p)|$ is calculated from the numerical spectrum data by dividing by the transition matrix elements $|\mathbf{d}| = |\langle 0|x|\mathbf{p}\rangle|$ with the $|\mathbf{p}\rangle$ obtained by numerically diagonalizing the field-free Hamiltonian $H_0 = \mathbf{p}^2/2 + V(x)$. The corresponding transition dipoles used in Fig. 1(a) are shown in Fig. 1(b) and will be discussed in detail below. The amplitude for H_2^+ in Fig. 1(a) is consistent with that of its reference atom in the high energy region but different in the low energy region, because it shows a pronounced peak structure, i.e., the amplitude of the peaks is one-order of magnitude higher.

We now extend these calculations to 2D. Fig. 2 plots the spectral amplitudes of 2D models of H_2^+ for varied molecular parameters and field intensities. The spectral amplitudes $|a(E_p)|$ are calculated from the numerical spectrum data by dividing by the transition matrix elements in the length gauge $|\mathbf{d}_{len}| = |\langle 0|\mathbf{r}|\mathbf{p}\rangle|$ with $|0\rangle$ obtained by the LCAO-MO approximation, and $|\mathbf{p}\rangle$ obtained by the plane wave approximation and the dispersion relation $\Omega = \mathbf{p}^2/2$ [14]. For $\theta = 90^\circ$, the spectral amplitudes of the models of H_2^+ and their corresponding reference atoms, which have been shifted vertically to compensate for differing the overall efficiency, are analogous (see Fig. 2(a) and (b)). However, for other angles, the most remarkable feature exhibited in Fig. 2(c)-2(f) is the peak structure at the electron kinetic energy that shifts rightward as the orientation angle increases. Except for these peaks, the spectral amplitudes of the other energy regimes are analogous. In addition, for the same orientation angle but different internuclear distance, the location of the peaks is shifted. For example, at $\theta = 50^\circ$, the peak is at $E_p = 1.85$ a.u. in Fig. 2(c), but it shifts

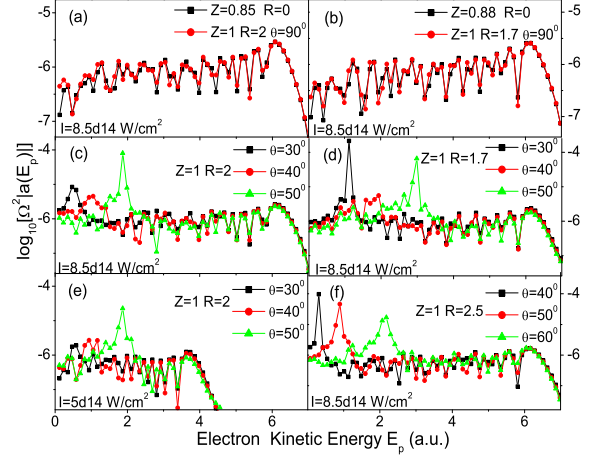


Figure 2: (Color online) The spectral amplitudes $\Omega^2 |a(E_p)| = \sqrt{S(\Omega)}/|\mathbf{d}_{len}|$ of 2D H_2^+ for varied molecular parameters and field intensities (indicated in each subpanel) calculated in the length gauge with the dispersion relation $\Omega = \mathbf{p}^2/2$. In Fig. 2(a) and 2(b), we also plot the $|a(E_p)|$ of those corresponding reference atoms for comparison.

to $E_p = 3$ a.u. in Fig. 2(d). For the same internuclear distance, at a fixed orientation angle the location of the peaks is almost unchanged when laser intensity varies, as revealed by Fig. 2(c) with $I = 8.5 \times 10^{14} \text{ W/cm}^2$ and 2(e) with $I = 5 \times 10^{14} \text{ W/cm}^2$. These calculations on 1D and 2D H_2^+ for diverse internuclear distance and laser intensities show that the spectral amplitudes of the molecules are usually dependent on the molecular orientation.

Next, we explain the mechanism behind these phenomena according to the Lewenstein model[16], where the time-dependent wave functions can be expanded under the strong-field approximation, $|\psi(t)\rangle = e^{iI_p t} [a(t)|0\rangle + \int d\mathbf{p} c_{\mathbf{p}}(t)|\mathbf{p}\rangle]$, where $a(t) \approx 1$ is the ground-state amplitude, and $c_{\mathbf{p}}(t)$ are the amplitudes of the corresponding continuum states, and can be written in the closed form

$$c_{\mathbf{p}}(t) = i \int_0^t dt' \mathbf{E}(t') \cdot \mathbf{d}(\mathbf{p} + \mathbf{A}(t) - \mathbf{A}(t')) \times e^{-i \int_{t'}^t [(\mathbf{p} + \mathbf{A}(t) - \mathbf{A}(t'))^2/2 + I_p] dt''}, \quad (2)$$

where $\mathbf{A}(t)$ is the vector potential of the laser field $\mathbf{E}(t)$. The time dependent dipole moment can be written as $\mathbf{D}(t) = \langle \psi_0(\mathbf{r}, t) | \mathbf{r} | \psi_c(\mathbf{r}, t) \rangle$, where $\psi_0(\mathbf{r}, t) = e^{iI_p t} |0\rangle$ denotes the initial electronic state and $\psi_c(\mathbf{r}, t) = e^{iI_p t} \int d\mathbf{p} c_{\mathbf{p}}(t) |\mathbf{p}\rangle$ denotes the REWP. Eq. 2 shows that the time-dependent continuum amplitude $c_{\mathbf{p}}(t)$ is not only dependent on the particular ionization potential I_p in the exponent of the integrand, but also depends on the ground state wave function through the transition dipole $\mathbf{d}(\mathbf{p})$ in the prefactor of the integrand. Thus, the continuum amplitudes of the molecule and its reference atom sharing the same ionization potential I_p

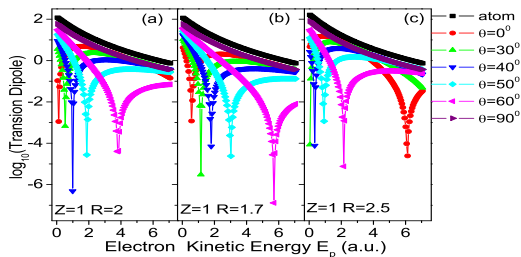


Figure 3: (Color online) The transition dipoles $|\langle 0|\mathbf{r}|\mathbf{p}\rangle|^2$ along the laser polarization direction of 2D H_2^+ with different R and orientation angles θ and their corresponding reference atoms, calculated in the length gauge with the dispersion relation $\Omega = \mathbf{p}^2/2$.

should have the same time-dependent phase, but their transition dipoles $\mathbf{d}(\mathbf{p})$ differ.

The above theoretical analysis has been checked by numerical simulation. For the 1D case, Fig. 1(b) clearly demonstrates that the transition dipole for H_2^+ is different from that for its reference atom. The transition dipole for H_2^+ shows a deep hollow (the amplitude of the hollow may be up to four order of magnitude lower) around $E_p = 0.33$ a.u., but is analogous with its reference atom in a broad higher energy region ($E_p = 1.5 \rightarrow 6$ a.u.). The ionization potential of H_2^+ is similar to its reference atom, and their transition dipoles also are analogous in a broad high energy region. Therefore, we expect that their spectral amplitudes $a(E_p)$, which are determined by $c_{\mathbf{p}}(t)$, also should be analogous in the high energy region, but different in the low energy region, as shown by Fig. 1(a). In addition, the location of the hollow in Fig. 1(b) corresponds to that of the peak in Fig. 1(a).

Fig. 3 shows the 2D transition dipoles used to produce Fig. 2. The transition dipoles for the reference atoms (the black curves in each subpanel of Fig. 3) are analogous, but the transition dipoles for the models of H_2^+ with different R show strong orientation dependence. The deep hollow moves as the angle θ changes. But, at $\theta = 90^\circ$, the transition dipoles for the models of H_2^+ are similar to that of the reference atoms in the energy region $E_p=0 \rightarrow 7$ a.u.. Thus we expect that, for $\theta = 90^\circ$, the spectral amplitude of H_2^+ should be identical with its reference atom, but for $\theta \neq 90^\circ$, they will show a large difference in the energy region where the deep hollow in the transition dipole of H_2^+ appears. This theory is verified by the plot in Fig. 2.

The 1D and 2D numerical results show that intrinsic properties of the molecules already enter the REWP. The deep hollows in the transition dipoles of H_2^+ with different θ can be read from the interference effect as predicted by Muth-Bohm *et al*[15]. Under the LCAO-MO approximation, the ground state of the diatomic molecule is $|0\rangle = \sum_i a_i |\phi_0(\mathbf{r} - \mathbf{R}/2)\rangle + b_i |\phi_0(\mathbf{r} + \mathbf{R}/2)\rangle$, where $|\phi_0(\mathbf{r})\rangle$ is the atomic ground state and a_i and b_i are the normal-

ization factors with $a_i = b_i$ for symmetric mixing and $a_i = -b_i$ for antisymmetric mixing. For symmetric mixing, e.g., H_2^+ , the transition dipole can be written as

$$\mathbf{d}(\mathbf{p}) = 2 \cos(\mathbf{p} \cdot \mathbf{R}/2) \sum_i a_i \mathbf{s}(\mathbf{p}) + i \mathbf{R} \sin(\mathbf{p} \cdot \mathbf{R}/2) \sum_i a_i \tilde{\phi}_0. \quad (3)$$

Here $\mathbf{s}(\mathbf{p}) = \int [e^{-i\mathbf{p}\cdot\mathbf{r}} \mathbf{r} \phi_0(\mathbf{r})] d\mathbf{r}$, $\tilde{\phi}_0(\mathbf{p}) = \int [e^{-i\mathbf{p}\cdot\mathbf{r}} \phi_0(\mathbf{r})] d\mathbf{r}$. The $\cos(\mathbf{p} \cdot \mathbf{R}/2)$ of the first term in Eq. 3 represents the interference between the two cores of the molecules[15], and the second term is proportional to the internuclear distance R in Eq. 3, leading to the breakdown of translation invariance. In our calculations, the second term is omitted according to Ref.[17, 18, 19]. Thus, the transition dipole of the molecule $\mathbf{d}(\mathbf{p})$ is different from that of the reference atom $\mathbf{s}(\mathbf{p})$ due to the interference effect from the term $\cos(\mathbf{p} \cdot \mathbf{R}/2)$. The interference that manifests itself as the hollows in the spectra of the transition dipole or the peaks in the HHG spectral amplitudes for the molecules, depends on the alignment angle θ and can be located by $pR \cos(\theta) = (2n + 1)\pi$ where n is an integer. For $R = 2$ a.u. and $\theta = 0^\circ$, the formula with the dispersion relation $\Omega = \mathbf{p}^2/2$ predicts the hollow location of $E_p = 0.12$ a.u., which is close to our numerical result of $E_p = 0.35$ a.u. in Fig. 1(b). If the dispersion relation $\Omega = \mathbf{p}^2/2 + I_p$ [14] is adopted, the location is estimated at $E_p = 1.23$ a.u., far away from the numerical result. We have calculated the dependence of the minima positions (in energy E_p) on molecular internuclear distance R in the 1D case. It shows that for the larger R (i.e., $R \geq 3$ a.u.) and larger momenta p (i.e., $p \geq 3$ a.u.), where the LCAO-MO approximation for the ground state $|0\rangle$ and the plane wave approximation for the continuum $|\mathbf{p}\rangle$ are expected to be more applicable, the above simple formula gives a good estimation on the location of the minima, i.e., the deviation is less than 1/10.

In addition, the transition dipoles for the reference atoms with different ionization potentials, as shown in Fig. 3(a) and 3(b), are almost identical. We attribute the difference in their HHG spectral amplitudes revealed by comparing Fig. 2(a) and 2(b) to the difference in their ionization potentials. The dependence of the spectral amplitude $a(E_p)$ on the ionization potential is also evident in the current theories of tunnel ionization (ADK[20], Yudin and Ivanov[21], MO-ADK[22]), where the ionization potential explicitly appears in the exponent of the formula determining the cycle dependence of the ionization rate. Thus, we expect that the time dependence of the continuum wave packet also relies on the ionization potential. Moreover, the present experiment for the orientation dependence of ionization rate of CO_2 shows a pronounced deviation from the prediction by the MO-ADK theory. The interference caused by the separated cores is not well described by the simple theory[23]. Thus, we expect that the dependence of the continuum wave packet on the HOMO is also not well described by the model. Based on this analysis, we conclude that due to the interference effect, the ionization and acceleration processes in the three-step model[24] also play an

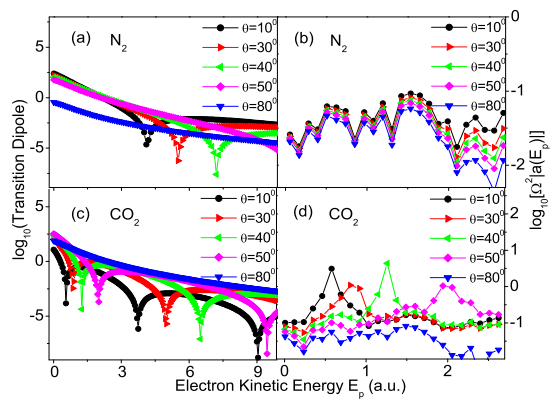


Figure 4: (Color online) The transition dipoles $|\langle 0|\mathbf{r}|\mathbf{p}\rangle|^2$ along the laser polarization direction ((a) and (c)) and spectral amplitudes $\Omega^2|a(E_p)| = \sqrt{S(\Omega)}|\mathbf{d}_{len}|$ ((b) and (d)) of N_2 and CO_2 with different orientation angles θ calculated in the length gauge with $\Omega = \mathbf{p}^2/2$. The laser intensity is $I = 2 \times 10^{14} \text{ W/cm}^2$ and wave length $\lambda = 800 \text{ nm}$. The orbitals of N_2 ($2p\sigma_g$) and CO_2 ($2p\pi_g$) are expressed in the LCAO-MO approximation.

important role in HHG from molecules. In fact, in our calculations, the hollows in Fig. 3 for molecules are responsible for the interference minima in harmonic spectra predicted by Lein *et al*[5].

This analysis demonstrates that the spectral amplitude of the molecular REWP is different from its reference atom due to the interference. However, why can the molecular orbital tomography experiment reconstruct the HOMO of N_2 by its reference atom Ar [9]? In Fig. 4, we plot the transition dipoles $|\mathbf{d}_{len}|^2 = |\langle 0|\mathbf{r}|\mathbf{p}\rangle|^2$ along the laser polarization direction ((a) and (c)) and the spectral amplitudes $|a(E_p)|$ ((b) and (d)) of N_2 and CO_2 with different orientation angles θ . The corresponding harmonic spectra are obtained by the Lewenstein model with the dispersion relation $\Omega = \mathbf{p}^2/2$ [9, 14]. For

N_2 with $R = 2.079 \text{ a.u.}$, the interference hollows at different angles θ should all appear in the high energy region, i.e., far away from the plateau regime. The curves of the transition dipoles in Fig. 4(a) are analogous to each other in the low energy region ($E_p \leq 2 \text{ a.u.}$). Accordingly, the spectral amplitudes in Fig. 4(b) also are analogous to each other in the same energy region within a vertical scaling factor. However, for CO_2 with $R = 4.38 \text{ a.u.}$, the curves of the transition dipoles in Fig. 4(c) show a large difference in the low energy region. The curves of the spectral amplitudes in Fig. 4(d) also are obviously different, showing a sharp peak shifting toward the higher energy region as the angle θ increases. We thus expect that the spectral amplitude for N_2 in the low energy region is largely independent of molecular orientation [9]. This conclusion is not applicable to CO_2 , for which the interference hollows for small orientation angles θ should appear in the lower energy region corresponding to lower harmonic orders in the plateau region[7, 8]. The spectral amplitude of CO_2 in that energy region is largely related to its orientation. Therefore, for some molecules, e.g., CO_2 , the interference effect should be included in the orbital tomography experiment to obtain an accurate HOMO wave function.

In summary, from our 1D and 2D numerical calculation and analytical deduction, we find that the assumption of the tomography method, i.e., that the recolliding electron wave packet of a reference atom may be used to extract the HOMO from high order harmonic spectra, may not be generalized to other molecules such as CO_2 . For these molecules, the molecular properties already enter the recolliding electron wave packet so the spectral amplitude of the molecular REWP shows a large difference from the reference atom and a strong orientation dependence in some energy regions due to the interference between the atomic cores of the molecule.

This work has been supported by NNSF Grant No. 10725521, CAEP Foundation Project No. 2006Z0202, 973 Research Project No. 2006CB806000, and by National Fundamental Research Programme of China under Grant Nos. 2006CB921400 and 2007CB814800.

-
- [1] R. Velotta *et al.*, Phys. Rev. Lett. **87**, 183901, (2001).
 - [2] J. Itatani *et al.*, Phys. Rev. Lett **94**, 123902, (2005).
 - [3] X. X. Zhou *et al.*, Phys. Rev. A **72**, 033412 (2005).
 - [4] C. B. Madsen and L. B. Madsen, Phys. Rev. A **74**, 023403 (2006).
 - [5] M. Lein *et al.*, Phys. Rev. Lett **88**, 183903, (2002); Phys. Rev. A **66**, 023805 (2002); M. Lein, *et al.*, *ibid.* **67**, 023819 (2003).
 - [6] G. L. Kamta and A. D. Bandrauk, Phys. Rev. A **71**, 053407 (2005).
 - [7] T. Kanai, S. Minemoto, and H. Sakai, Nature **435**, 470(2005).
 - [8] C. Vozzi *et al.*, Phys. Rev. Lett. **95**, 153902 (2005).
 - [9] J. Itatani *et al.*, Nature **432**, 867(2004).
 - [10] S. Patchkovskii *et al.*, Phys. Rev. Lett.**97**, 123003, (2006).
 - [11] R. Torres *et al.*, Phys. Rev. Lett. **98**, 203007, (2007).
 - [12] Van-Hoang Le *et al.*, Phys. Rev. A **76**, 013414 (2007).
 - [13] S. Patchkovskii *et al.*, J. Chem. Phys.**126**, 114306 (2007).
 - [14] J. Levesque *et al.*, Phys. Rev. Lett. **98**, 183903(2007).
 - [15] J. Muth-Bohm, A. Becker, and F. H. M. Faisal, Phys. Rev. Lett. **85**, 2280(4) (2000)
 - [16] M. Lewenstein, Ph. Balcou, M. Yu. Ivanov, Anne L' Huillier, and P. B. Corkum, Phys. Rev. A **49**, 2117(1994).
 - [17] J. Chen and S. G. Chen, Phys. Rev. A **75**, 041402(R) (2007).
 - [18] D. B. Milosevic, Phys. Rev. A **74**, 063404 (2006).
 - [19] W. Becker *et al.*, Phys. Rev. A **76**, 033403 (2007).
 - [20] M. V. Ammosov, N. B. Delone and V. P. Krainov, Sov.

- Phys. JETP **64**, 1191(1986).
- [21] Gennady L. Yudin and Misha Yu. Ivanov, Phys. Rev. A **64**, 013409 (2001).
- [22] X. M. Tong, Z. X. Zhao, and C. D. Lin, Phys. Rev. A **66**, 033402 (2002).
- [23] D. Pavičić *et al.*, Phys. Rev. Lett. **98**, 243001 (2007).
- [24] P. B. Corkum, Phys. Rev. Lett. **71**, 1994(1993).